Academic Science Journal

Synthesis of ZnO: Cu and Ag Bimetallic Nanoparticles by Laser Ablation

Amer M. Hussein*, Jasim M. Mansoor and Ammar A. Habeeb

Department of Physics – College of Science – University of Diyala

*amerm0296@gmail.com

Received: 14 August 2023 **Accepted: 28 September 2023**

DOI: https://dx.doi.org/10.24237/ASJ.02.04.797C

Abstract

Nanoparticles (ZnO: Ag and Cu) were prepared using the pulsed laser ablation method in liquid. The prepared samples were characterized by X-ray diffraction patterns (XRD), particle size analysis (PSA), UV-visible spectroscopy, and Zeta potential (ZP). the JCPDS standard card for Zn (01-080-0074) validated the hexagonal ZnO structure by X-ray diffraction for (ZnO) and (ZnO: Cu and Ag). we calculated the average crystal size of all the produced samples, and we observe that the crystal size grows as the ratio of copper and silver doping rises. The UV-VIS results showed excellent absorption bands of 290–345 nm, confirming that the Ag-containing nanocomposites absorb visible light. As a result, the spectral absorption band of pure ZnO widens with the adding of Cu and Ag, and the absorption edge moves towards a longer wavelength. This significant increase in absorption in the visible region indicates that the generated nanocomposites can reach a more significant catalytic activity in the visible region. The energy gap value decreases, namely 2.97, 2.90, 2.87, 2.79, 2.65, and 2.488 eV, respectively, due to the increasing doping ratio of silver and copper. ZP data of colloidal solutions containing (ZnO) and (ZnO: Ag and Cu) nanoparticles exhibits negative values indicating increased stability of the nanoparticles. However, the ZP data was found to be dependent on the concentration of the surfactant, with an increase in the zeta potentials value corresponding to an increase in the concentration of the surfactant. The PSA results showed promising outcomes and the absence of nanoparticle agglomeration. The synthesized particles were analyzed using

Academic Science Journal

FESEM and IMAGE J software to indicate if the particles were nano-sized. Additionally, the particles spherical and quasi-spherical shapes were investigated and found to be of minimal nanoscale size.

Keywords: Bimetallic nanoparticles, ZnO, Cu, Ag, doping, laser ablation, Energy gap

تحضير الجسيمات النانوية ثنائية المعدن ZnO: Cu – Ag عن طريق الاستئصال بالليزر في السائل

عامر محمد حسين و جاسم محمد منصور و عمار عايش حبيب

قسم الفيزياء – كلية العلوم – جامعة ديالى

الخلاصة

تميزت الجسيمات النانوية (ZnO: Ag and Cu) المحضرة بطريقة الاستئصال بالليزر النبضي في السائل بواسطة (PSA) و(XRD) والتحليل الطيفي المرئي للأشعة فوق البنفسجية (UV-vis) و (ZP) و (FESEM). من نتائج (XRD) تم التحقق من صحة بطاقة JCPDS القياسية لـ Zn (01-080-0074) من صحة بنية ZnO السداسية عن طريق حيود الأشعة السينية لـ (ZnO) و (ZnO: Cu و Ag). قمنا بحساب متوسط حجم البلورات لجميع العينات المنتجة ولاحظنا أن حجم البلورات ينمو مع ارتفاع نسبة النحاس والفضة. من نتائج UV-VIS للجسيمات النانوية (ZnO: Ag and Cu) كانت نطاقات الامتصاص مميزة من (290-345) نانومتر, يتضح في هذه النتيجة أن المركبات النانوية المحتوية على Ag تمتص الضوء المرئي. نتيجة لذلك يتسع نطاق الامتصاص الطيفي لأوكسيد الزنك (ZnO) النقي بإضافة Cu و Ag وتتحرك حافة الامتصاص باتجاه طول موجي أطول تشير هذه الزيادة الكبيرة في الامتصاص في المنطقة المرئية إلى أن المركبات النانوية المتولدة يمكن أن تصل إلى فعالية تحفيزية أكبر في المنطقة المرئية. تتناقص قيمة فجوة الطاقة ؛ أي 2.97 , 2.90 , 2.87 , 2.79 , 2.65 , 2.488 فولت على التوالي وهذا هو تأثير زيادة نسبة المنشطات من الفضة والنحاس. من نتائج ZP للقيم المحتملة لزيتا حصلنا عليها لجميع المحاليل الغروية المحضرة حيث نلاحظ أن القيم الموجبة التي هي اكبر من (30+) والقيم السالبة التي هي اقل من (30-) تشير إلى مزيد من الاستقرار للجسيمات النانوية ومع ذلك فإن قيمة إمكانات زيتا تعتمد على تركيز المادة الخافضة للتوتر السطحي حيث أن زيادة تركيز الفاعل بالسطح تزيد من قيمة جهد زيتا. من نتائج PSA لـ (ZnO) و (ZnO: Ag and Cu) أظهرت قيم حجم الجسيمات في المحاليل الغروية المحضرة نتائج جيدة وعدم وجود تكتل للجسيمات النانوية. من نتائج FESEM كانت الجسيمات التي حصلنا عليها ضمن المقياس النانوي ولها أشكال كروية وشبه كروية وأحجام نانوية صغيرة جدًا.

الكلمات المفتاحية : الجسيمات النانوية ثنائية المعدن، اوكسيد الزنك، النحاس، الفضة، التشويب، الاستئصال بالليزر، فجوة طاقة.

Academic Science Journal

Introduction

Pure zinc oxide is a chemical compound of zinc, found in nature as a white solid that changes color to orange upon heating due to retinal deformations, it is a semiconductor with the chemical symbol ZnO, which is non-toxic and insoluble in water. It dissolves in mineral acids [1]. Zinc oxide is employed in various electronic devices, including high-power electronics, surface wave acoustic devices, capacitors, piezoelectric transducers, pneumatic sensors, and UV emitters [2]. The definition of laser ablation is the ejection of material from a surface under low- and high-intensity laser pulses (PLAL), and the rate of ablation, which gives the maximum thickness of the sample ablated during laser pulse irradiation, describes the process efficiency [3]. With laser ablation technology, different laser sources can fabricate NPS nanoparticles from infrared to ultraviolet light, while the pulse duration ranges from 10ns-10fs during laser ablation in liquids. The laser pulse passes through the transparent liquid layer at the laser wavelength and melts the target surface. Thus, the thin liquid layer near the melt surface will be heated to a high temperature and expand over the melt, expelling it into the surrounding liquid; when the metal particles are removed, the solute that was disseminated in the solvent is still a colloidal component of the NPS suspensions, and the laser radiation is then absorbed by the free electrons, which subsequently diffuse energy into the material [4-5]. From a scientific and technological perspective, more attention has been shown in bimetallic nanoparticles than in monometallic nanoparticles. The metals that make up bimetallic nanoparticles and their nanometric scale dictate their characteristics. These are created by fusing metallic nanoparticles with different architectural structures. They tend to increase the energy of the metal combinations absorption band, giving us a flexible biosensing instrument. Size-dependent optical, electrical, thermal, and catalytic effects may be among these features, which are different from those of pure elemental particles [6].

The present study focuses on the synthesis of bimetallic colloidal nanoparticles consisting of zinc oxide (ZnO), copper (Cu), and silver (Ag) using the process of laser ablation.

1. Experimental Procedure

For preparing a colloidal solution of ZnO: Ag and Cu bimetallic nanoparticles using pulsed laser ablation, the following steps were used:

a) The raw materials of (ZnO) and (ZnO: Cu and Ag) nanoparticles were prepared by the sol-gel method, and its characterizations of results were sent to the publication in another Journal)—the weight ratios of prepared NPs are shown in Table 1.
b) The prepared NPs were pressed with a hydraulic press at 3.5 Tons of pressure for 5 minutes using a mold with a diameter of 1.6 cm to prepare circle targets. The amount of each sample was 1.5 grams.
c) After pressing, A targets were sintered at 1000 degrees Celsius to get a hard target.
d) The targets were placed in the bottom of a 5 mL round glass beaker filled with 3 mL of deionized water.
e) During the ablation phase, the vessel was moved around itself; the target was placed 13 cm away from the laser lens, and the laser parameters are a frequency of 1 Hz, a wavelength of 1046 nm, a laser power of 600 mJ, and 550 pulses. The colloidal solution of the nanoparticles is obtained.
f) Steps 1 to 5 are repeated six times. We obtained the colloidal solution of the nanoparticles.

x-ray diffraction patterns (XRD), particle size analysis (PSA), UV-visible spectroscopy, Zeta potential (ZP), UV-VIS spectroscopy, and field emission scanning electron microscopy (FESEM) were used for analyzing prepared colloidal solutions of the nanoparticles.

Table 1: The weight ratios of the prepared samples.

Sample	Zn%	Ag%	Cu%	W=Zn	W=Ag	W=Cu	W=Citric Acid
Z1	100	0	0	22.31175	0	0	7.88025
Z2	95	2.5	2.5	21.19616	0.312956	0.738435	
Z3	90	5	5	20.08058	0.625913	1.47687	
Z4	85	7.5	7.5	18.96499	0.938869	2.215305	
Z5	80	10	10	17.8494	1.251825	2.95374	
Z6	75	12.5	12.5	13.38705	1.564781	3.692175	

Results and Discussion

a) X-Ray Diffraction Results

XRD analysis was performed to determine the exact crystal structure, and crystalline size of the Nano composites. The XRD patterns of the as prepared Nano composites (Z1, Z2, Z3, Z4, Z5 and Z6) as shown in figure 1, reveal well-defined diffraction peaks at 31.73°, 34.38°, 36.22°, 47.48°, 56.54° and 62.77° Indexed as (100), (002), (101), (102), (110), (103) quartzite hexagonal planes of the ZnO phase, in agreement with JCPDS Card No. ZnO (01-076-0704) [7]. However, the powders (Z2, Z3, Z4, Z5 and Z6) reveal the appearance of peaks for CuO at 35.55°, 38.05°, 57.98°, 62.01°, 32.14°and 45.63° belonging to (-111), (111), (-113), (110) and (-112) having mono crystal structure according to the standard JCPDS Card No. (01-080-0076) [8]. which increases its intensity decreases with decreasing full width at half maximum and increasing doping rate. (Z2, Z3, Z4, Z5 and Z6) produces deflection peaks at 62.81°, 64.30° and 65.6°associated with (220), (022) and (110) level. Return to its monoclinic conforming to the standard card JCPDS Card No. AgO (01-074-1743) [9]. From the relation of Scherer's Formula, the crystallite size was calculated by increasing the concentration of Ag, the position of the peak is shifted towards lower values, as shown in figure 1. This shift indicates a partial replacement of Ag+ ions in the ZnO lattice and an increase in the lattice a and c scales, as expected [10]. This subject pertains to the examination of the ionic size density among Ag+ ions (0.126 nanometer) as well as Zn+2 ions (0.074 nm) within the ZnO lattice, specifically focusing on the overlapping of Ag ions., which slows down the crystallization of the host as a result of the formation of oxygen voids due to the difference in the ionic diameter between them. This makes a decrease in the crystal size. As for an increase in the concentration of Cu, it did not have a significant effect on the host, Zn, because the ionic diameters of both are very close, since the ionic diameter is Cu+2 (0.073) nm. Moreover, there was no substantial alteration in the depiction of the summits. The phenomenon of diffraction is observed when a separation of Ag ions occurs within the lattice structure of ZnO, hence preventing their replacement for ZnO sites [11]. The presence from AgO and CuO phases, shown by the minor shift in the peak positions of the ZnO phase, provides evidence for the successful production of

ZnO nanocomposites. The observed decreased crystal size Table 2, as determined by the application of the Scherrer and William Hall equation:

$$D=k\,\lambda/\beta\cos\theta \quad \ldots \quad (1)$$

Where K represents the shape factor and its value lies between (1-0.9) depending on the shape of the grains, (λ) represents the wavelength of the X-ray, (β) represents the full width at half maximum the curve at intensity to the middle (FWHM) and (θ) represents the diffraction angle.

$$B\cos\theta = k\,\lambda/D_{W\text{-}H} + [4\,\varepsilon\sin\theta] \quad \ldots \quad (2)$$

Since (ε): micro- strain and ($D_{W\text{-}H}$) particle size (nm), (β) Full width at half maximum peak (rad), (θ) The angle of incidence of x-rays (degree), (k) is a constant of approximately (0.9).

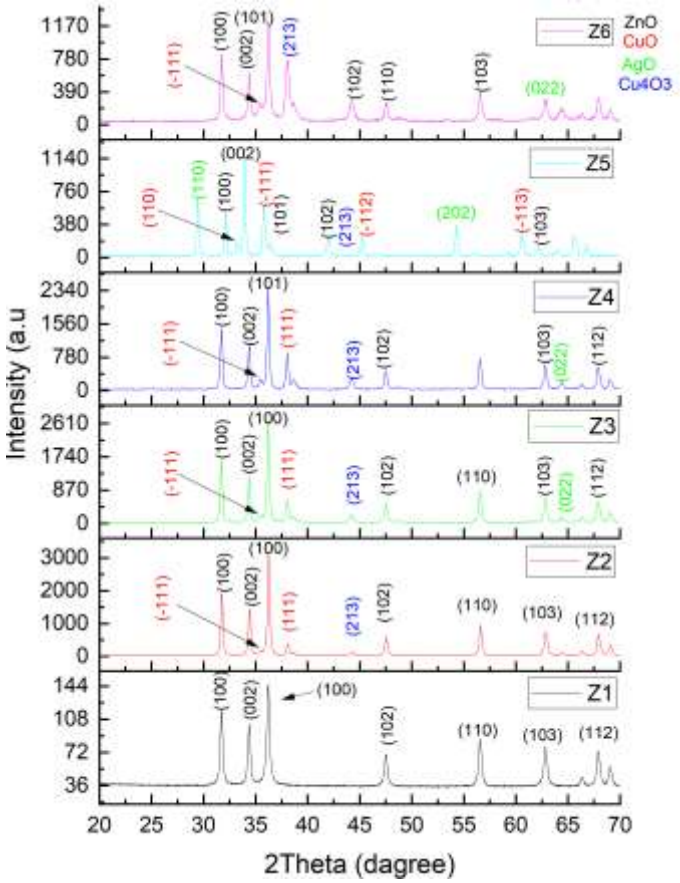

Figure 1: X-ray diffraction pattern of (ZnO) and (ZnO: Cu – Ag) nanoparticles.

Table 2: crystal size D_{101} (nm) Average and Crystallite size WH of (ZnO) and (ZnO: Cu - Ag) nanoparticles.

Samples	Crystallite size Average (nm)	Crystallite size (nm) WH
Z1	25.49	33.82
Z2	22.94	29.32
Z3	22.40	28.91
Z4	25.29	32.70
Z5	26.11	34.37
Z6	20.27	27.79

b) Zeta Potential Results

This measurement was done to determine the presence of agglomerates in the solutions and to investigate the stability of the materials created by the pulsed laser ablation process at various concentrations. The zeta potential is essential for determining how stable colloidal scattering. When neighboring particles with the same charge scatter, the size of the zeta potential gauges how strongly electrostatic attraction exists between them. The forces of attraction might outweigh the forces of repulsion when the potential is low. Therefore, electrically dispersing colloids had high zeta potential, either positive or negative, and coagulating, aggregating, or agglomerating colloids had low zeta potential [12]. When the zeta potential values range from higher than (+30 mV) to lower than (-30 mV), the stability criteria of NPs can be assessed [13]. In Figure 2, zeta potential distributions are displayed in the produced colloidal nanoparticles. Table 3 shows the values of zeta potentials that we obtained for all the prepared colloidal solutions, where we note variations in the values of ZP from positive to negative values between (15.95 to -44.08) indicating that prepared samples have low and high stability. However, the zeta potential value depends on the surfactant's concentration and the period of preparations, as increasing the surfactants concentration increases the zeta potential value [14].

Academic Science Journal

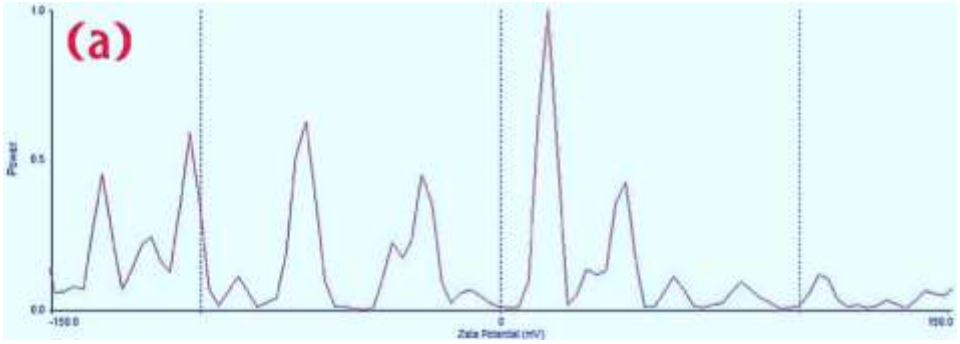

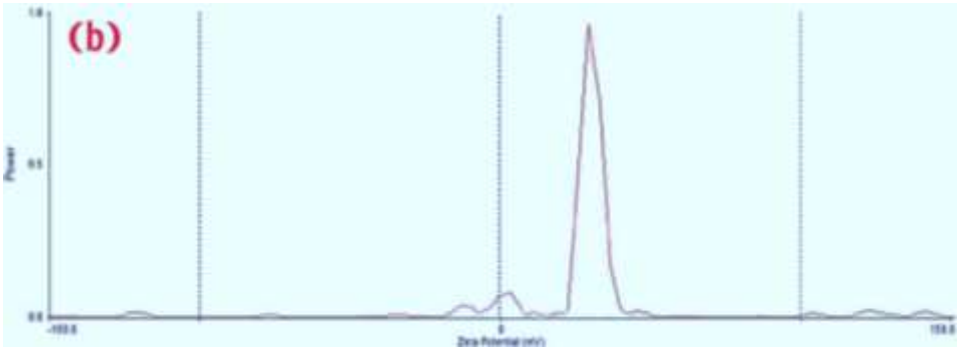

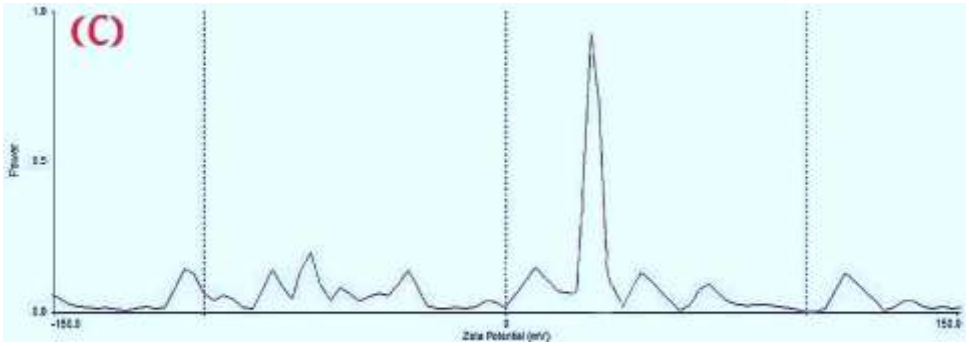

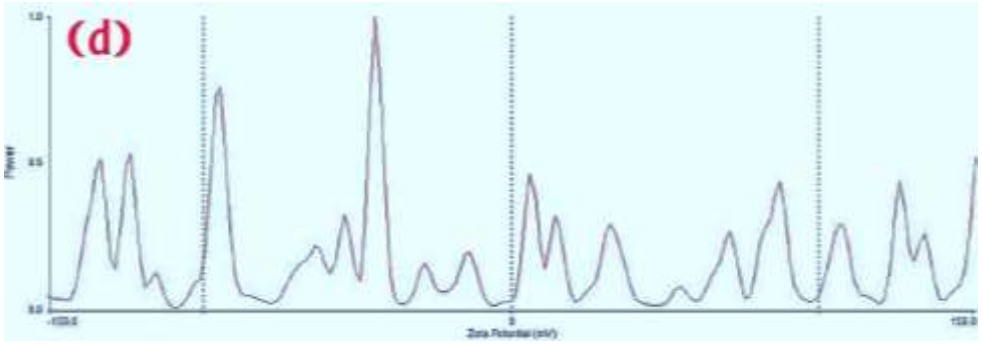

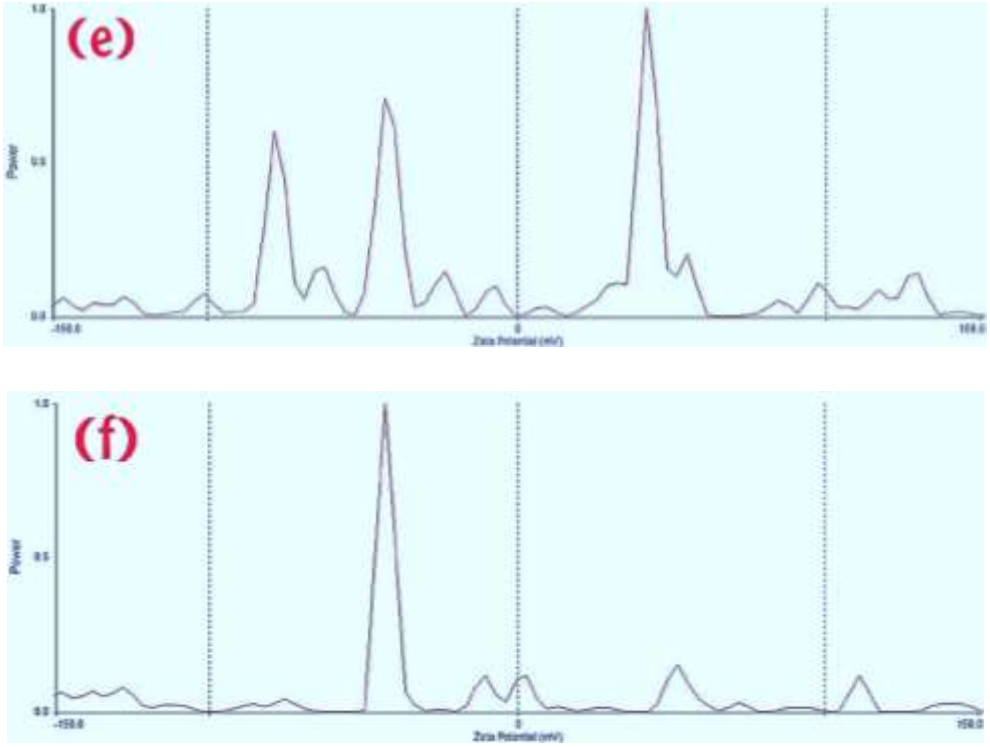

Figure 2: Plots of Zeta Potential of solutions of colloidal (ZnO) and (ZnO: Cu - Ag) nanoparticles**.**

Table 2: Values of Zeta Potential of solutions of colloidal (ZnO) and (ZnO: Cu - Ag) nanoparticles.

SAMPLE	ZETA POTENTIAL (MV)
Z1	15.95
Z2	33
Z3	30.68
Z4	-44.08
Z5	42.07
Z6	-42.92

c) Particle Size Analyser (PSA)

Particle size and particle size distribution can be measured in several ways. Others rely on ultrasound, an electric field, gravity, or centrifugation. Some are light-dependent. In all techniques, volume is a measure determined indirectly by a model that transforms the particles actual shape into an abstract shape, such as a sphere or a cube (when using the least square

method). One of the most widely used techniques for particle size detection is laser diffraction, which analyzes the light scattering pattern in a sample to calculate the particle size distribution (PSA). An array of sensors monitors and measures the scattering pattern produced when light interacts with particles. It is possible to determine particle size from the scattered light of a mathematically observed sample since the angle and intensity of the scattering pattern are proportional to particle size. The fraction size distribution of the measured particle field diameter of equivalent size is used to provide the particle size information for a given sample [15]. Figure 3 shows the results of measuring the particle size prepared by the pulsed laser ablation method in the liquid. Table 4 shows the particle size values in the prepared colloidal solutions, which showed promising results and little aggregation of the nanoparticles.

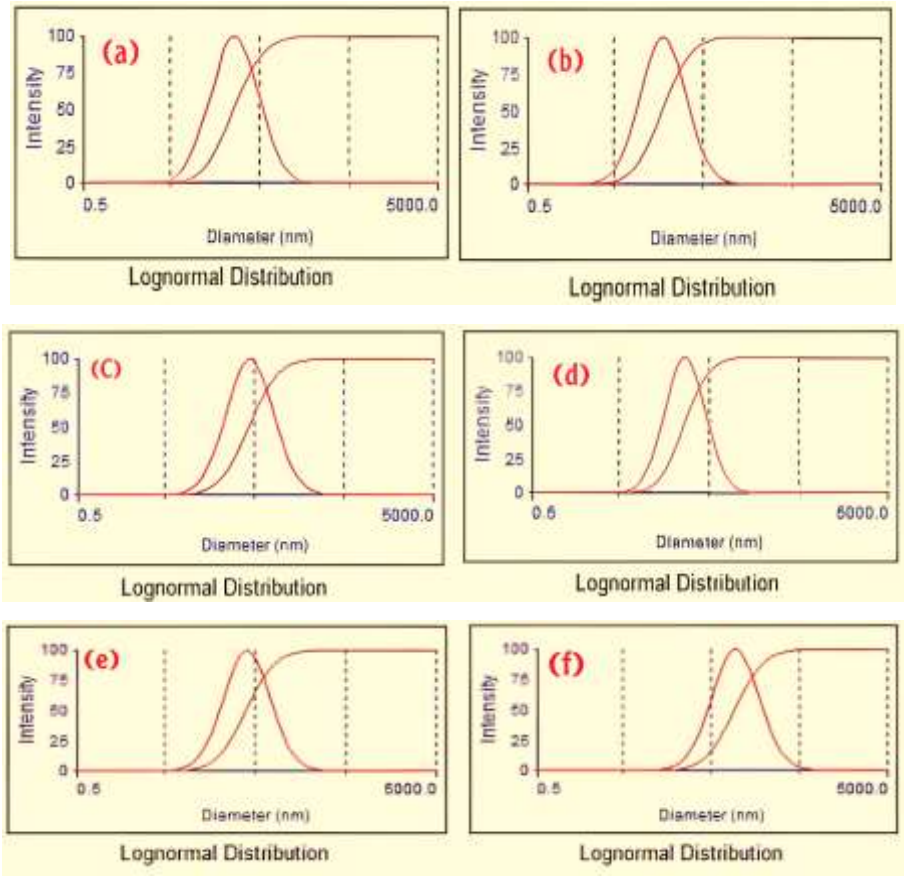

Figure 3: Particle Size Analysers of solutions of ZnO and (ZnO: Cu – Ag) colloidal nanoparticles.

Academic Science Journal

Table 4: Particle Size Analyzers of solutions of ZnO and (ZnO: Cu - Ag) colloidal nanoparticles.

samples	Particle Size (nm)
Z1	31.5
Z2	19.4
Z3	43.9
Z4	29.5
Z5	39.9
Z6	93.5

d) Field Emission Scanning Electron Microscopy (FESEM) Results

The surface morphology of the produced colloidal solutions was examined after placing them on a quartz slide and letting them dry completely. Nanoparticle sizes were calculated using (image J) software. average sizes of nanoparticles, and standard deviation. Figure 4 shows the results of the FESEM examination of FESEM nanoparticles prepared by pulsed laser ablation in liquid. The particles obtained were within the nanoscale and had spherical and semi-spherical shapes, and very small nanosized. The mean values of size (nm) for metal nanoparticles created using the pulsed laser ablation technique in liquid and the standard deviation are displayed in Table 5.

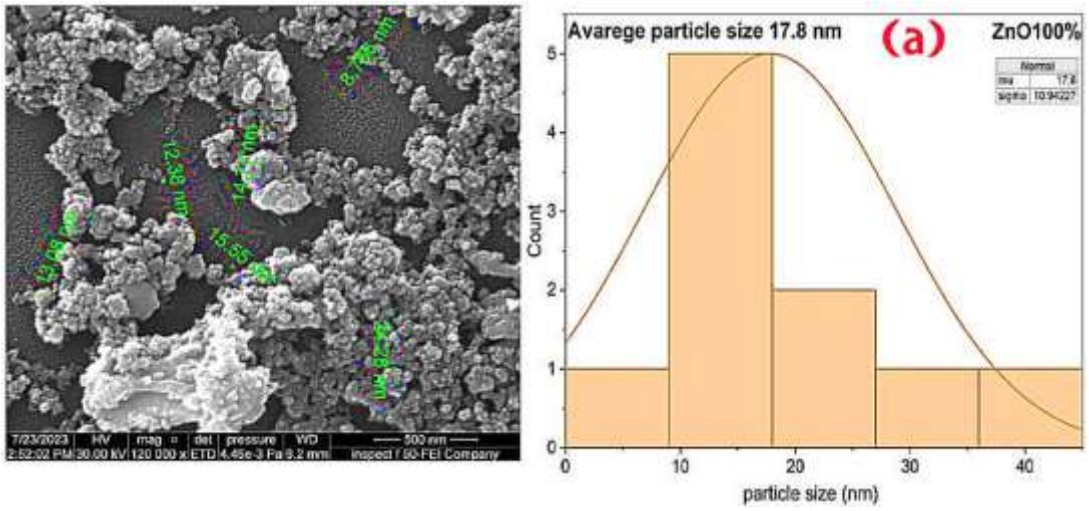

Academic Science Journal

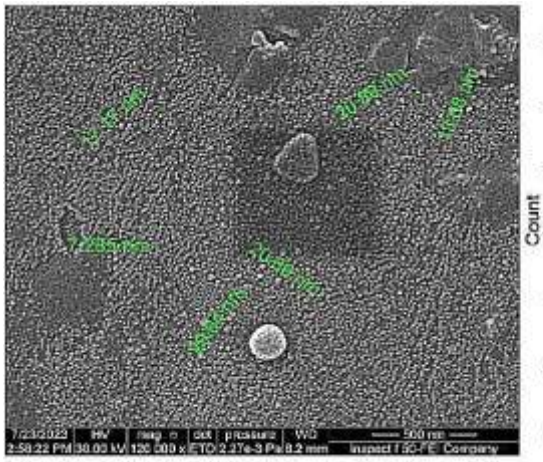

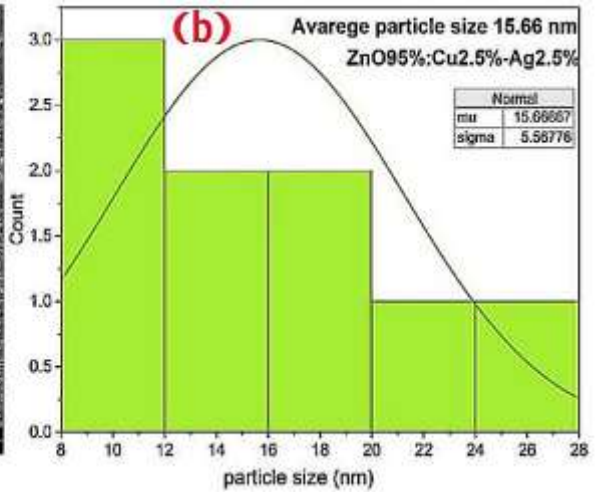

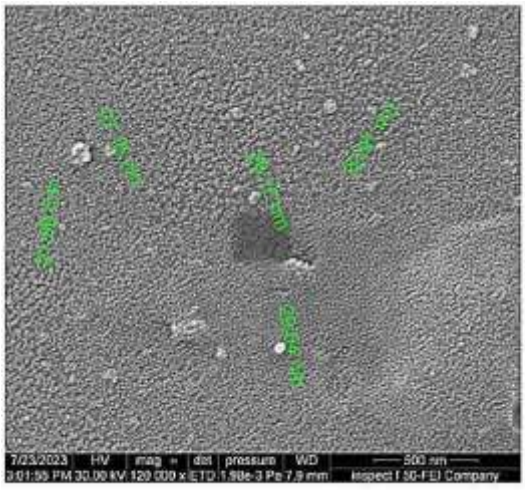

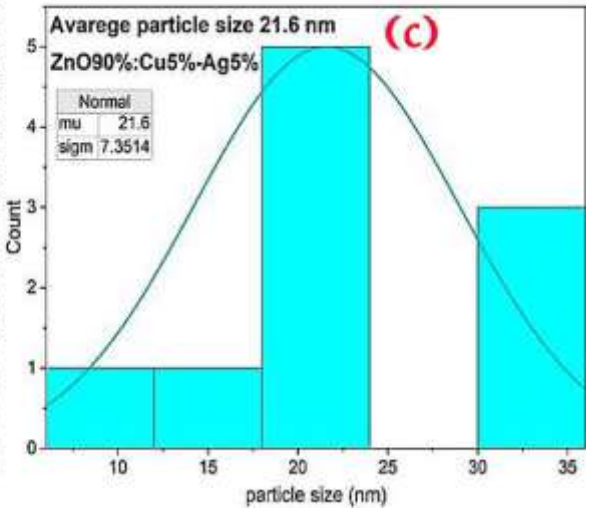

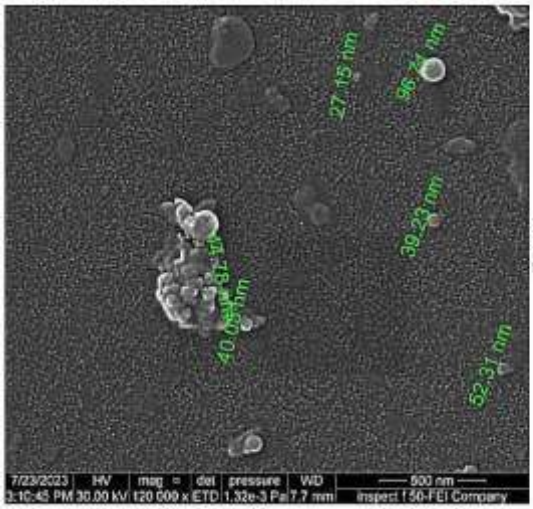

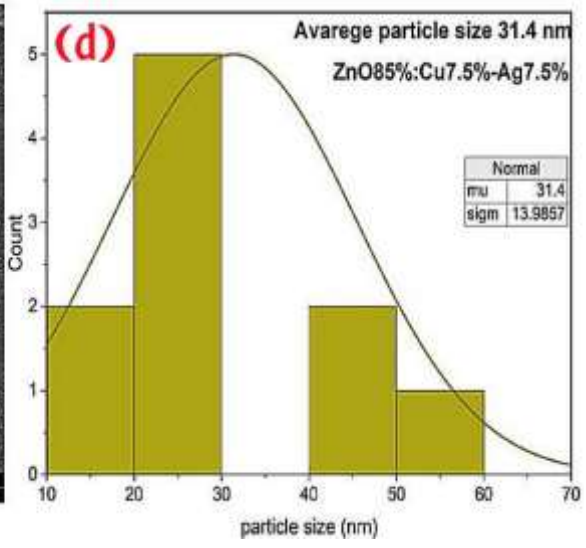

Academic Science Journal

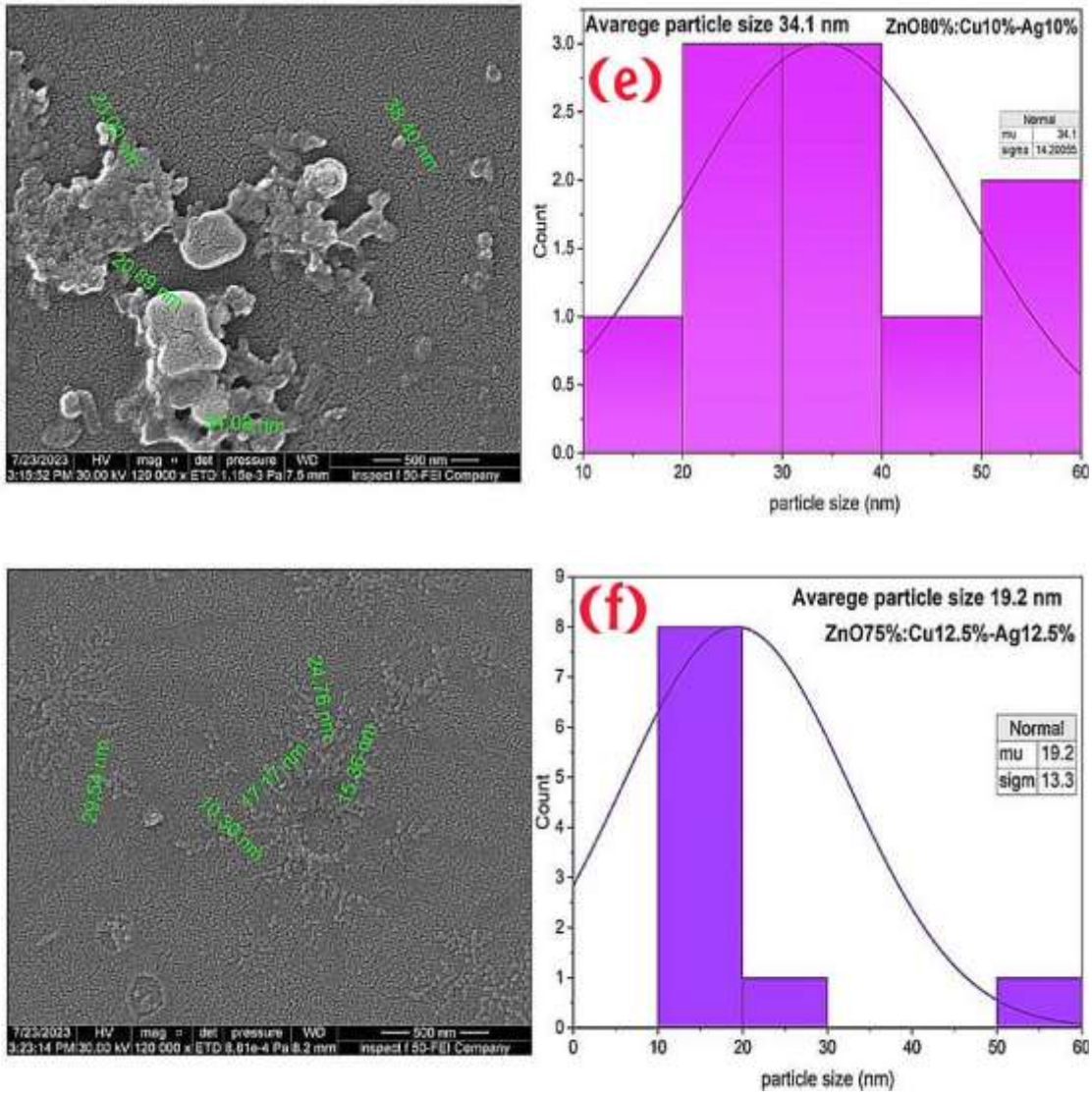

Figure 4: FESEM images (a, b, c, d, e and f) of ZnO and (ZnO: Cu - Ag) nanoparticles.

Table 5: Standard Deviation and Average Size of FESEM images of ZnO and (ZnO: Cu - Ag) nanoparticles.

NANOPARTICLES TYPES	STANDARD DEVIATION	AVERAGE SIZE (NM)
Z1	10.94	17.8
Z2	5.56	15.6
Z3	7.35	21.6
Z4	13.98	31.4
Z5	14.2	34.1
Z6	13.3	19.2

e) Optical Properties Results

1. Absorbance and optical energy gap

For ZnO nanoparticles maintained at consistent temperatures and filled with binary fillers generated by pulsed laser ablation in liquid, absorption at a wavelength range (300–1100 nm) was estimated. Because the relationship between wavelength and photon energy is inverse, transfer electrons from the valence bands to the conduction bands. The zinc oxide and zinc oxide doped with Cu and Ag nanoparticles UV-vis spectra revealed discrete absorption bands between 290 and 345 nm. While considering the well-known surface plasmon, this discovery proves that Cu and Ag-containing nanocomposites absorb visible light [16]. As a result, when Ag and Cu are added to (pure ZnO), the spectral absorption band broadens and the absorption edge shifts towards a protracted wavelength. This substantial increase in visual absorption suggests that the created nanocomposites can reach greater visible catalytic efficacy [17].

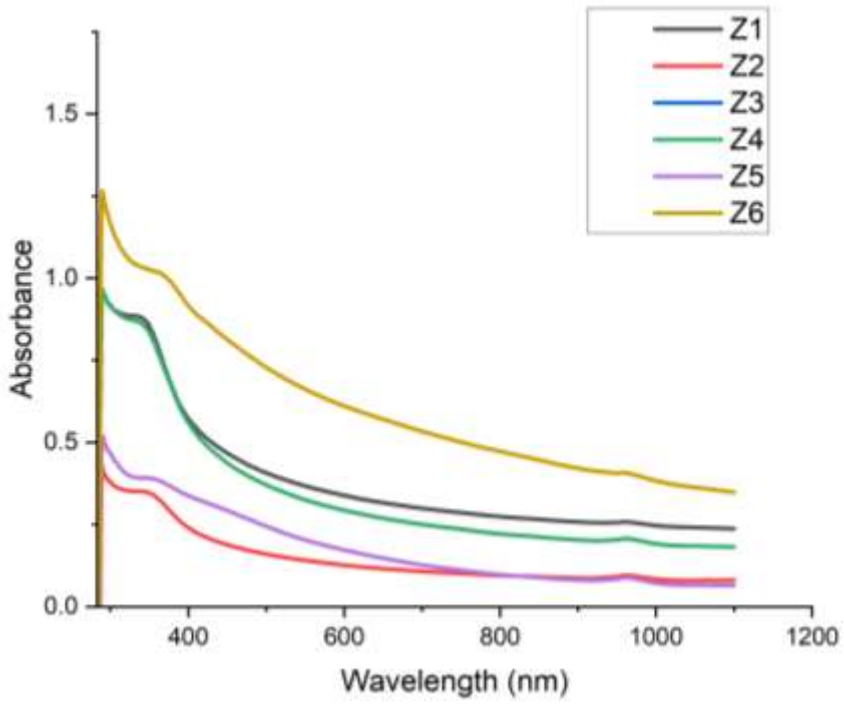

Figure 5: UV-Visible absorption spectra of solutions of ZnO and (ZnO: Cu - Ag) colloidal nanoparticles samples.

Academic Science Journal

The optical energy gap for direct transmission of the pulsed laser ablation-prepared nano solutions (Z1, Z2, Z3, Z4, Z5, and Z6) in the liquid was calculated, as shown in Figure 4. The chemical bonds between the elements that make up its structure, the size of its grains, and general fluctuations (e.g., with change in particle size) all have a significant impact on the energy gap, as indicated by the gap values obtained by plotting the relationship between $(\alpha h\upsilon)^2$ and (E).

$$(\alpha hv)^{1/n} = A\,(hv - Eg) \qquad (1)$$

Where, h is the Planck constant, ν is the frequency, α is the absorption coefficient, Eg is the bandgap energy, A is the proportionality constant, and n denotes the type of electronic transition (for directly allowed transitions, n = 1/2). As seen in Figure 5, the energy gap value drops with values of 2.97, 2.90, 2.87, 2.79, 2.65, and 2.488 eV, respectively. As can be observed, the value of pure ZnO NPs (2.97 eV) is significantly lower than that of bulk ZnO (3.37 eV). Band gap narrowing often occurs when particle size is decreased to the nanoscale and is linked to a quantum confinement effect. Additionally, the two primary mechanisms that contribute to the reduction in band gap energy with Ag-Cu co-dopings are (i) the shape of the particle formation CuO-ZnO nanoparticles decorated with Ag, or (ii) the use of Zn sites to partially replace Cu and Ag ions within the ZnO host lattice [18].

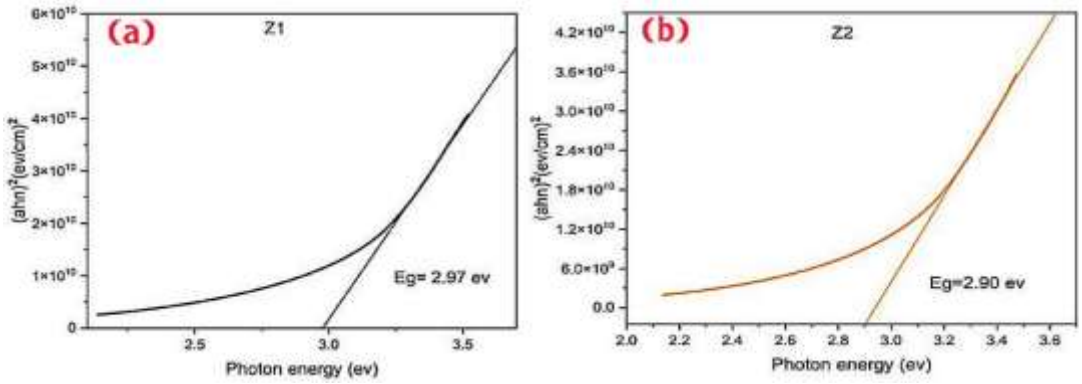

Academic Science Journal

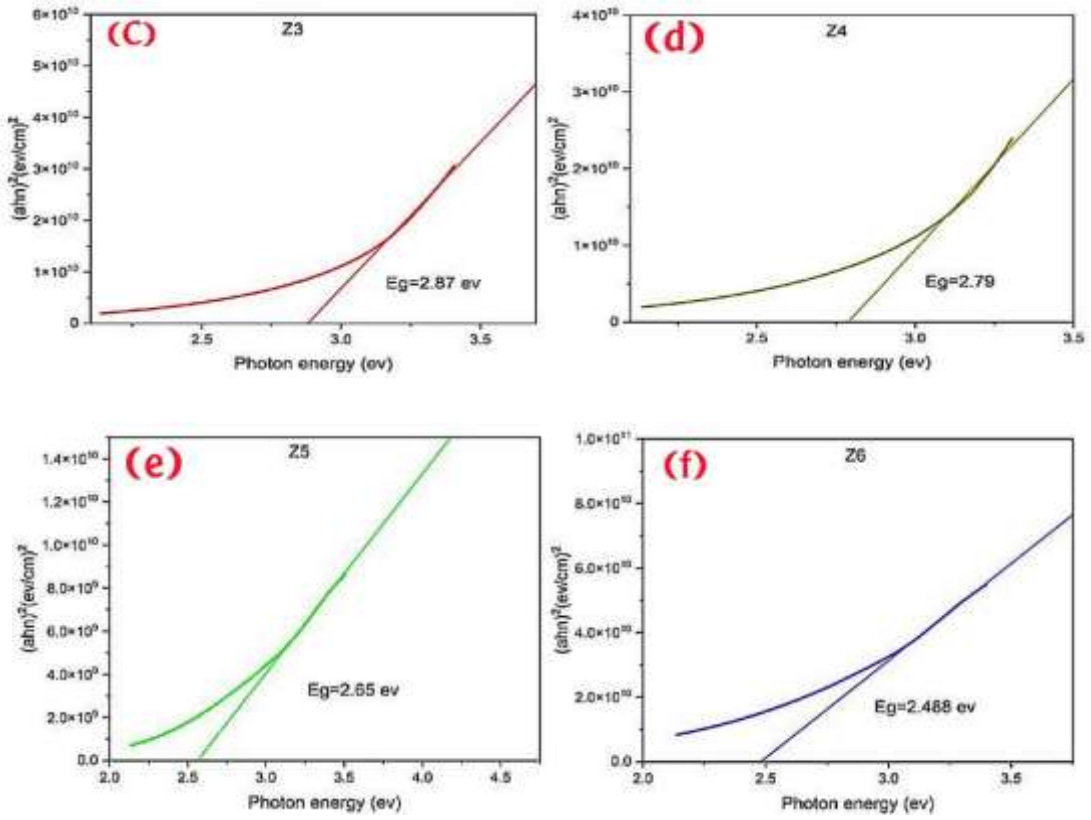

Figure 6: Direct band gap estimations of solutions of ZnO and (ZnO: Cu - Ag) Colloidal nanoparticles by laser ablation in liquid samples.

Table 6: Optical energy gap of solutions of ZnO and (ZnO: Cu - Ag) colloidal nanoparticles samples.

SAMPLES	OPTICAL ENERGY GAP (EV)
Z1	2.97
Z2	2.90
Z3	2.87
Z4	2.79
Z5	2.65
Z6	2.488

Conclusions

We have successfully prepared ZnO doped with silver and copper using the pulsed laser ablation method in liquid with different weight ratios. The pulsed laser ablation in distilled water as a liquid medium is suitable for forming colloidal ZnO and ZnO: Ag and Cu nanoparticle solutions, the location and intensity of the surface plasmon resonance can determine the ablation efficiency. The higher the concentration of the colloidal solution, the greater the absorption intensity, X-ray diffraction patterns showed that both the doped and undoped ZnO NPs formed in a hexagonal wurtzite structure, the zeta potential tests colloidal solutions of (ZnO: Cu and Ag) were unstable colloidal in general. UV Visible Spectrum - Show distinct absorption bands from 290 to 345 nm with redshift in the absorption peaks, the PSA test for colloidal solutions (ZnO: Cu and Ag) showed promising results and some agglomeration. FESEM results showed that small nanoparticles with spherical and semi-spherical shapes were obtained.

References

1. H. Hartnagel, Semiconducting transparent thin films, (1995).
2. S. R. Manalis, S. C. Minne, C. F. Quate, Atomic force microscopy for high-speed imaging using cantilevers with an integrated actuator and sensor, Applied Physics Letters, 68(6), 871-873(1996)
3. S. Y. Yang, S. G. Kim, Characterization of silver and silver/nickel composite particles prepared by spray pyrolysis, Powder Technology, 146(3), 185-192(2004)
4. D. Blázquez Sánchez, The surface plasmon resonance of supported noble metal nanoparticles: characterization, laser tailoring, and SERS application (Doctoral dissertation), (2007)
5. K. Zimmer, Analytical solution of the laser-induced temperature distribution across internal material interfaces, International journal of heat and mass transfer, 52(1-2), 497-503(2009)

6. G. Sharma, A. Kumar, S. Sharma, M. Naushad, R. P. Dwivedi, Z. A. ALOthman, G. T. Mola, Novel development of nanoparticles to bimetallic nanoparticles and their composites: A review, Journal of King Saud University-Science, 31(2), 257-269(2019)
7. G. Muruganantham, K. Ravichandran, K. Saravanakumar, K. Swaminathan, N. J. Begum, B. Sakthivel, Effect of solvent volume on the physical properties of sprayed fluorine-doped zinc oxide thin films, Crystal Research and Technology, 47(4), 429-436(2012)
8. A. Gnanaprakasam, V. M. Sivakumar, M. Thirumarimurugan, A study on Cu and Ag doped ZnO nanoparticles for the photocatalytic degradation of brilliant green dye: synthesis and characterization. Water Science and Technology, 74(6), 1426-1435(2016)
9. V. Vaiano, M. Matarangolo, J. J. Murcia, H. Rojas, J. A. Navío, M. C. Hidalgo, Enhanced photocatalytic removal of phenol from aqueous solutions using ZnO modified with Ag. Applied Catalysis B: Environmental, 225, 197-206(2018)
10. C. Karunakaran, V. Rajeswari, P. Gomathisankar, Combustion synthesis of ZnO and Ag-doped ZnO and their bactericidal and photocatalytic activities, Superlattices and Microstructures, 50(3), 234-241(2011)
11. F. Sun, X. Qiao, F. Tan, W. Wang, X. Qiu, One-step microwave synthesis of Ag/ZnO nanocomposites with enhanced photocatalytic performance, Journal of Materials Science, 47, 7262-7268(2012)
12. M. F. Meléndrez, G. Cárdenas, J. Arbiol, Synthesis and characterization of gallium colloidal nanoparticles, Journal of Colloid and Interface Science, 346(2), 279-287(2010)
13. A. B. García, A. Cuesta, M. A. Montes-Morán, A. Martínez-Alonso, J. M. Tascón, Zeta potential as a tool to characterize plasma oxidation of carbon fibers, Journal of colloid and interface science, 192(2), 363-367(1997)

14. S. K. Misra, A. Dybowska, D. Berhanu, S. N. Luoma, E. Valsami-Jones, The complexity of nanoparticle dissolution and its importance in nanotoxicological studies, Science of the total environment, 438, 225-232(2012)
15. A. Jillavenkatesa, S. J. Dapkunas, L. S. H. Lum, Particle Size Characterization, Special Publication 960-1. Natl. Inst. Stand. Technol., Washington, US Government Printing Office, 2001)
16. T. Liu, B. Liu, L. Yang, X. Ma, H. Li, S. Yin, Y. Wang, RGO/Ag2S/TiO2 ternary heterojunctions with highly enhanced UV-NIR photocatalytic activity and stability, Applied Catalysis B: Environmental, 204, 593-601(2017)
17. T. M. Althagafi, A. F. Al Baroot, M. Grell, A new precursor route to semiconducting zinc oxide, IEEE Electron Device Letters, 37(10), 1299-1302(2016)
18. O. M. Ntwaeaborwa, S. J. Mofokeng, V. Kumar, R. E. Kroon, Structural, optical and photoluminescence properties of Eu3+ doped ZnO nanoparticles, Spectrochimica Acta Part A: Molecular and Biomolecular Spectroscopy, 182, 42-49(2017)